Available online at www.sciencedirect.com

ScienceDirect

materialstoday: PROCEEDINGS

Materials Today: Proceedings 2 (2015) 629 – 636

12th European Conference on Thermoelectrics

# Electronic properties of Bi-Sn diluted alloys

Fedotov A.S.[a*], Svito I.A.[a], Gusakova S.V.[a], Shepelevich V.G.[a], Saad A.[b], Mazanik A.V.[a], Fedotov A.K.[a]

[a]*Belarusian State University, Nezavisimosti av., 4, 220030, Minsk, Belarus*
[b]*Al-Balqa Applied University, P.O. Box 2041, Amman 11953, Salt, Jordan*
** fedotov@bsu.by*

**Abstract**

The dependences of resistivity, magnetoresistance, Hall effect and thermoEMF in the 4 – 300 K temperature range and in magnetic fields up to 8 T were studied for the $Bi_{1-x}Sn_x$ ($0 \le x \le 0.006$) diluted alloys produced by the melt spinning method. The observed decrease of conductivity and magnetoresistance with doping is explained in terms of charge carriers scattering on tin atoms, whereas the shift of the Hall and Seebeck coefficients to the range of positive values is connected with enhanced contribution of holes in the charge transport.


Selection and peer-review under responsibility of Conference Committee members of the 12th European Conference on Thermoelectrics.

*Keywords:* Bismuth, Stanum, polycrystalline foils, resistivity, Hall effect, Seebeck effect, magnetoresistance.

## 1. Introduction

Thermoelectric materials (TEM) are widely used for production of electric current generators and fabrication of Peltier coolers. Among existing industrial TEMs for medium-temperature range (up to 400 – 450 °C) generators, bismuth based alloys and compounds are the most common. In recent years, there is a demand for micro-miniature film type generators and coolers which can operate not only at elevated temperatures, but at temperatures significantly below room. Such devices are needed for temperature control and stabilization in integral circuits and other systems operated at low temperatures. For such purposes the bismuth-containing alloy films may be used.


Selection and peer-review under responsibility of Conference Committee members of the 12th European Conference on Thermoelectrics.
doi:10.1016/j.matpr.2015.05.088

The other problem is that thermoelectric elements of standard construction require both p- and n-type materials. TEM of p-type with sufficient thermoelectrical figure-of-merit are much harder to fabricate. In addition, conventional industrial TEMs of p-type usually being fabricated with Te, which is one of the rarest elements in the Earth crust. So the problem of good p-type TEM is still open. Bi alloys with Sb and Sn show some good result in this field [1].

In terms of price-to-quality ratio, polycrystalline bismuth-based films are probably most suitable for these purposes. Concerning their heating/refrigeration applications, we discuss below the situation from point of view of their figure-of-merit $ZT = S^2T\sigma/\kappa$ [2-3]. In this equation, $\sigma$ is the electrical conductivity, $\kappa$ is the thermal conductivity, $S$ is the Seebeck coefficient, and $T$ is the temperature. Therefore, to increase the $ZT$ values, we need to have larger Seebeck coefficient $S$, higher electrical conductivity $\sigma$ and lower thermal conductivity $\kappa$.

As is known, the thermal conductivity has both electron and phonon components ($\kappa = \kappa_e+\kappa_{ph}$). The electronic component $\kappa_e$ is related to the $\sigma$ value through the Wiedemann–Franz law $\kappa_e=L\sigma T$ ($L$ is the Lorenz factor), and increases with the electrical conductivity growth. The phonon component $\kappa_{ph}$ depends on the lattice imperfections. In bulk semiconducting TEMs, such as Bi-based alloys, $\kappa_{ph}$ is larger than $\kappa_e$. Therefore, if $\kappa_{ph}$ is decreased by structural modification, the overall thermal conductivity can be decreased and the figure-of-merit increased, since this change can be made without significantly affecting $\sigma$ and $\kappa_e$.

Approaches to decrease the phonon component of the thermal conductivity include methods to increase the number of phonon scattering sites, such as interfaces introduced by reduction the size and/or dimensionality of TEMs, namely, using thin films (2-dimension) [4-5], wires (1-dimension) [6-7], or by decreasing the grain size in film materials [2].

One can infer from the above discussion that there is a potential to increase $ZT$ values in Bi-based alloy films by modifying their grain structure to enhance the effectiveness of phonon scattering. Specifically, TEM should have a structure consisting of small grains (from micro- to nanoscales) which have a high degree of crystallographic orientation: the c-direction of all the grains should be aligned and all the basal planes parallel, while misorientations of the basal planes between grains should be supplied by rotation about the c-axis [3]. Such crystallographic texture will result in a low phonon conductivity in the basal plane and an enhanced $ZT$, while the electrical properties will affected insufficiently.

Note also that polycrystalline bismuth-based alloy films are attractive for studying not only from practical point of view, but also form scientific standpoint, because even many types of bismuth binary alloys films are not well understood compared with similar studies of single crystals.

So, the main goal of presented study was to investigate temperature/magnetic field dependences of thermoelectric and galvanomagnetic properties of diluted $Bi_{1-x}Sn_x$ alloy foils prepared by the melt spinning technique.

## 2. Experimental

For fabrication of the studied foils we used Bi and Sn of 99.9999 % purity. Bi and Sn were melted, mixed and poured out on the cold surface of a polished copper cylinder with 20 cm diameter rotating with a frequency of about 1200 rpm. Foil cooling rate can be estimated from the formula:

$$U = \frac{a \cdot \theta}{C \cdot D \cdot t}, \tag{1}$$

where $a$ is the heat convection coefficient, $\theta$ is the excessive temperature of the melt, $C$ is the specific heat capacity of the melt, $D$ is the bismuth density, $t$ is the foil thickness. Heat convection coefficient for a polished copper surface can be estimated as $(1 – 2)\cdot10^5$ W/(m$^2$·K) [8]. Excessive temperature of the melt was 100 K. Taking into account the $a$ value for copper, and also $\theta$, $C$ and $D$ for Bi, the cooling rate for foils was estimated as $10^6 – 10^7$ K/s for the thickness of 30 – 60 μm. Cooling rates of the same order were reported by other researchers for similar experiments [8,9]. The set of foils with atomic concentration of Sn equal to 0, 0.12, 0.25 and 0.6 at. % was produced.

Temperature and field dependences of resistivity, magnetoresistance (MR), Hall effect and thermoEMF were measured in the 4 – 300 K temperature range and in magnetic fields up to 8 T using a Cryogen Free Closed-Cycled Measuring System (Cryogenic Ltd., London).

Current through the sample was passed using a Keithley 6430 SourceMeter, which allows to set current with 0.05 % precision and to measure sample resistance in the range from 100 μΩ to 20 GΩ. Sample temperature during measurements of electrical properties was controlled by a LakeShore 340 system equipped with Cernox CX-1030-SD sensors providing accuracy better than 0.05 K.

For measurements of resistivity $\rho$, Hall coefficient $R_H$ and MR, the rectangular samples (2 x 10÷15 mm) with two current, two potential and two Hall contacts deposited by ultrasound soldering of indium were fabricated. Clamping bronze contacts were used for measurement of thermoEMF. The sample was placed in a special measuring cell involving thermometers, magnetic field sensors and heaters to control the temperature. The measuring cell was inserted into a superconducting solenoid inside of the cryostat.

Magnetoresistance was measured in magnetic field perpendicular to the current direction. ThermoEMF was measured in magnetic fields parallel to the temperature gradient. All measurements were done under DC regime. Resistivity and Hall effect were measured by the 4-probes potentiometric method and the 4 switching method, respectively. The temperature difference on the sample during thermoEMF measurements was equal to 1.5±0.1 K.

The relative error for DC measurements did not exceed 5 % for resistivity (it was determined mainly by the error of sample sizes and interprobe distance determination), 0.1–0.2 % for MR and 0.5–1 % for $R_H$. Measurement error of the Seebeck coefficient $S$ did not exceed 2 % above 200 K and 10 % at helium temperatures (2–10 K).

Surface morphology and grain structure of the studied foils were investigated with a LEO 1455VP scanning electron microscope (SEM) equipped by an attachment for the study of electron backscatter diffraction (EBSD). Foil surface was slightly polished before EBSD experiments. The thickness ranging in 60 ± 5 μm was estimated on cleavages of the foils studied using SEM with an accuracy of ~ 3–4 %.

## 3. Results and Discussion

### *3.1. Structure*

As the used Sn concentrations did not exceed the solubility limit in Bi [10], no additional phases in the studied Bi – Sn foils were detected. The scanning electron microscopy and electron diffraction studies have shown polycrystalline structure of the foils with a mean grain size close to 20 μm (Fig. 1).

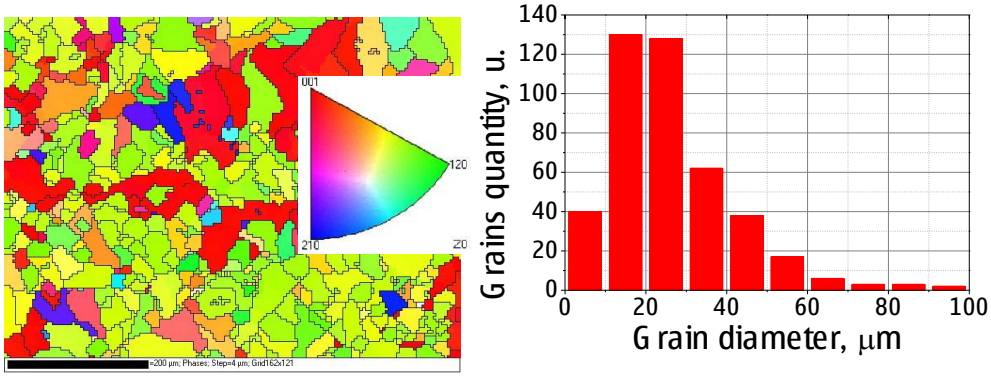


Fig. 1. Example of typical grain structure (a) and grain size distribution (b) for the $Bi_{0.9988}Sn_{0.0012}$ foils

EBSD studies have shown that the textures of the Bi – Sn alloys are very similar to those of the pure bismuth foils (Fig. 2). Straight poles in Fig. 2 are given in hexagonal lattice system. Data were taken with 4 μm step, numbers in braces are indices of corresponding crystallographic plane.

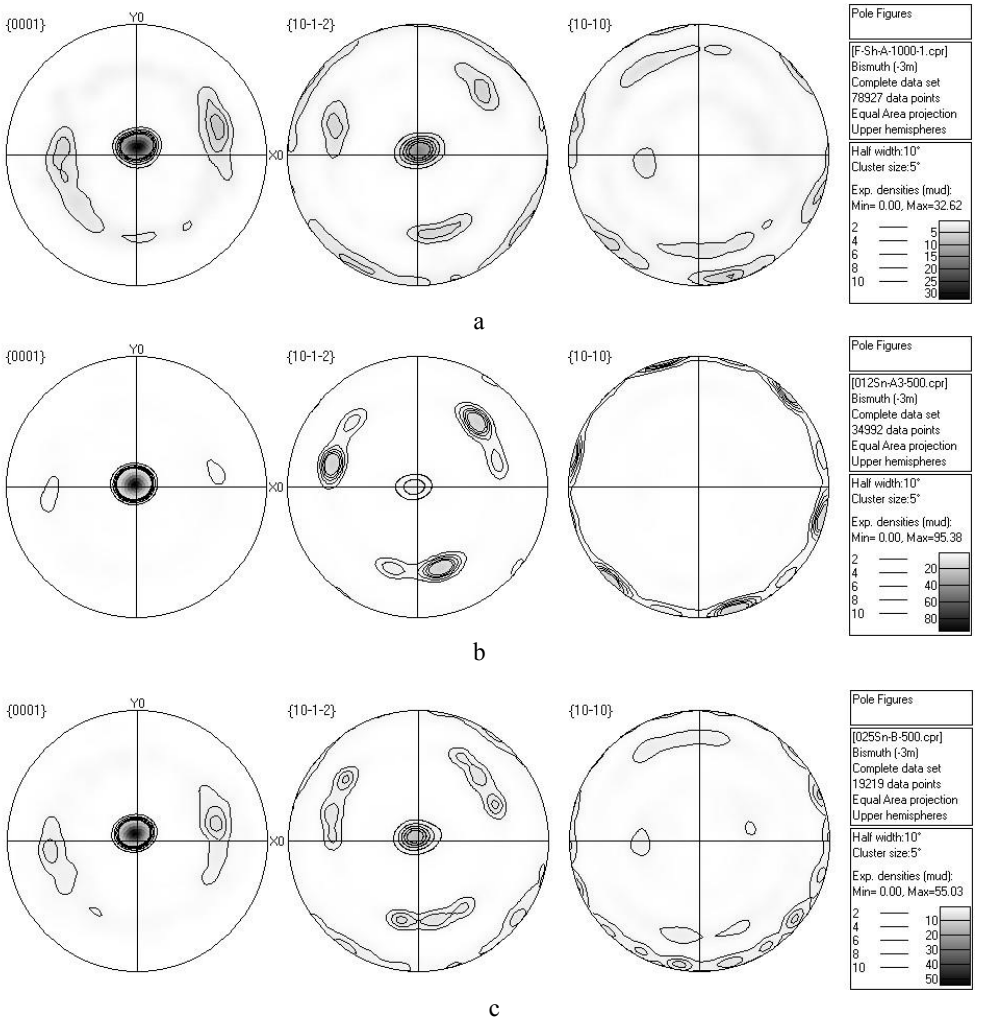


Fig. 2. Pole figures for the pure bismuth (a), $Bi_{0.9988}Sn_{0.0012}$ (b) and $Bi_{0.9975}Sn_{0.0025}$ (c) foils

### *3.2. Electron transport properties*

When analyzing electron transport properties of the Bi – Sn alloys, it is necessary to take into account that incorporation of tin atoms to bismuth leads to change of both carriers concentration and their mobilities. The valence of bismuth differs from the valence of tin by a unit, so tin acts as acceptor. Besides changing of carriers concentration, tin atoms also act as scattering centers influencing the carriers mobility. The last effect is determined by the temperature and doping level because it depends on the state of impurities (charged or neutral).

As is seen from Fig. 3, in the studied $Bi_{1-x}Sn_x$ diluted alloys the $\rho(T)$ curves are close to linear, i.e. the temperature dependences of resistivity show metallic behavior. In so doing, resistivity is increased with doping relative to the pure bismuth foils that probably indicates the enhanced influence of scattering on dopants on electron transport in the foils.

Fig. 4 presents field dependences of relative magnetoresistance $MR(B) = [\rho(B)-\rho(0)]/\rho(0)$, which are also changed ambiguously with doping. Note main features of the $MR(B)$ dependences for different $x$ and $T$ values. As experiments have shown, at low temperatures (Fig. 4a) in low magnetic fields magnetoresistance depends on $B$ very similar for the pure and Sn doped Bi foils nonmonotonous. Doping suppresses magnetoresistance of $Bi_{1-x}Sn_x$ foils at $B = 8$ T by about 3 – 4 orders depending on the temperature. At $T > 10$ K MR decreases monotonously with doping

level (Figs. 4b-d).

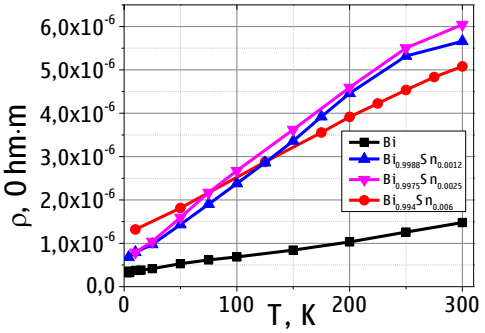


Fig. 3. Temperature dependences of resistivity ρ(*T*)

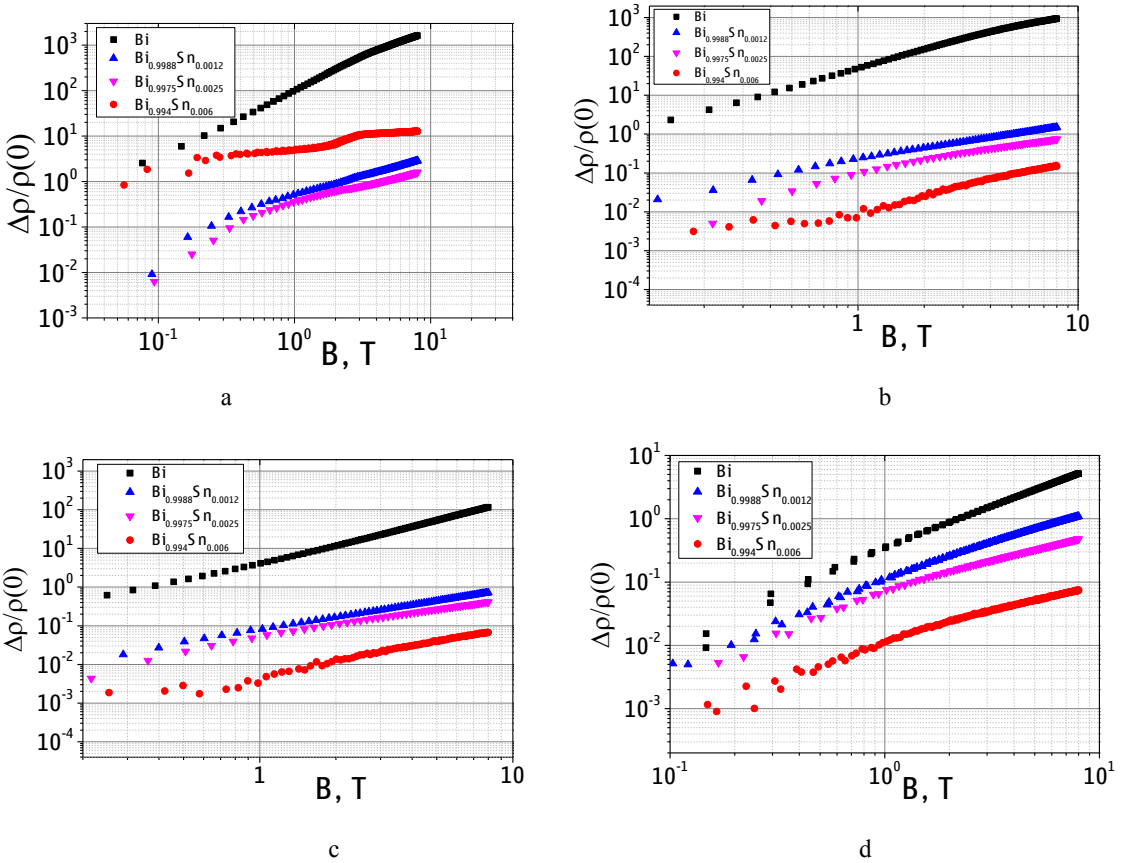


Fig. 4. Field dependence of relative magnetoresistance MR(*B*) at 4 K (a), 50 K (b), 150 K (c), 250 K (d)

Magnetoresistance in bismuth-like samples is usually being described by the Lorentz mechanism. The longer mean free path of a charge carrier, the more curved it's trajectory (until it transforms to cycloid when mean free length path becomes much longer than cyclotron radius). Additional scattering centers (tin atoms) decrease mean free path and charge carrier doesn't have enough time between collisions to react on magnetic field. In the simplest case it leads to decrease of relative magnetoresistance with increase of dopant concentration.

Figs. 5 and 6 present temperature dependences of Hall and Seebeck coefficients for different *x* and *B* values. As

is seen, the pure Bi foils display a negative sign both for the $R_H(T)$ and $S(T)$ dependences at the whole temperature range confirming dominant electron contribution to carrier transport. Absolute values of $R_H$ tend to zero at high temperatures at all magnetic fields (Fig. 5). As is seen, Sn doping of the Bi foils results in the shift of $R_H(T)$ and $S(T)$ curves to the range of positive values (Fig. 5, Fig. 6) due to an enhanced participation of holes in carrier transport. As is seen, the Hall coefficient is positive in the whole range of the studied temperatures and magnetic fields.

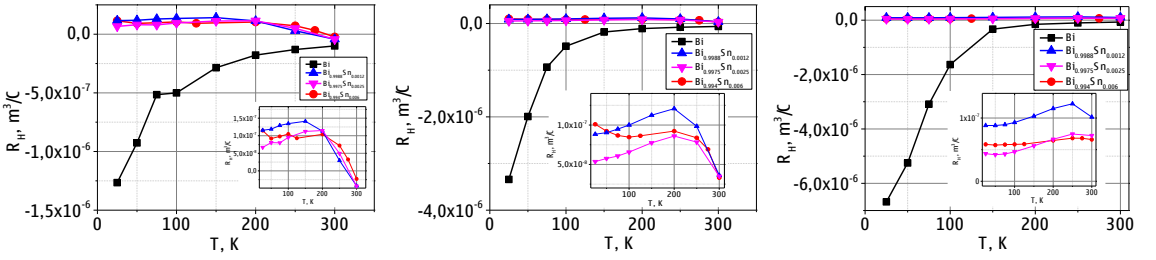


a b c

Fig. 5. Temperature dependence of Hall coefficient $R_H(T)$ at $B$ = 0.25 T (a), $B$ = 1.75 T (b) and $B$ = 8 T (c).

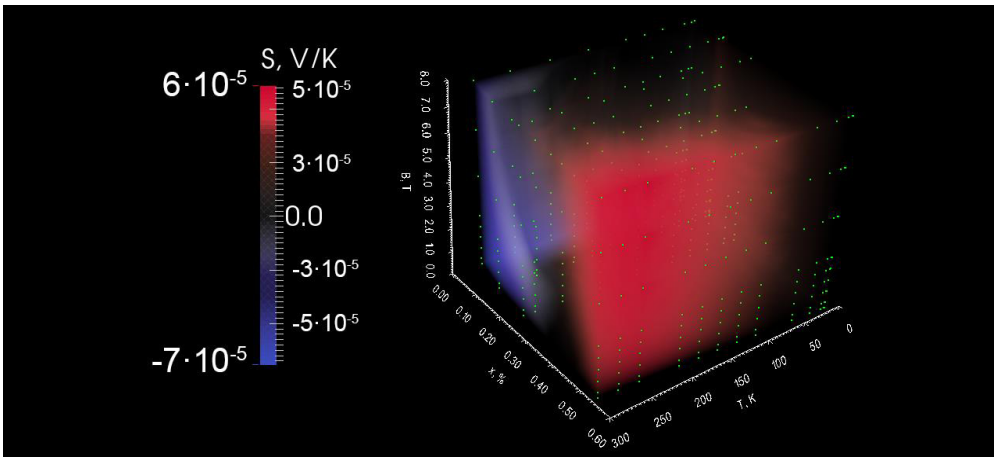


a

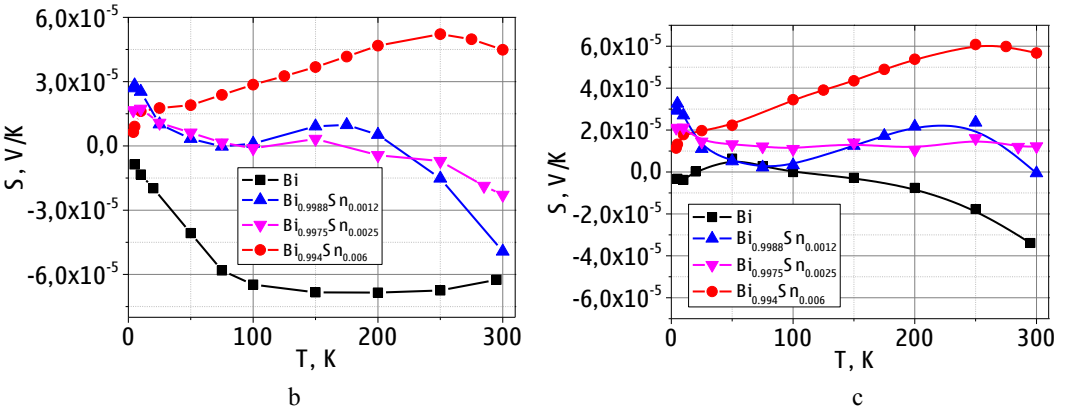


b c

Fig. 6. Seebeck coefficient depending on Sn concentration $x$, temperature $T$, and magnetic field $B$ (a); $S(T)$ at $B$ = 0 T (b); $S(T)$ at $B$ = 8 T (c). In Fig. 6a green dots present experimental values, volume mapping is obtained by the Delaunay triangulation using a ParaView software.

An introduction of tin in bismuth leads to following changes of band structure (Fig. 7). Fermi level goes down

with increase of dopant concentration. This leads to dominance of holes at low temperatures and explains shift of Hall and Seebeck coefficient to positive values [12]. The increase of electron concentration with temperature determines the fact that the Hall coefficient of doped samples decrease by absolute value at room temperature (Fig.5). Because mobility of L-electrons is significantly higher than one of T-point holes, electrons are affected by magnetic field stronger than holes.

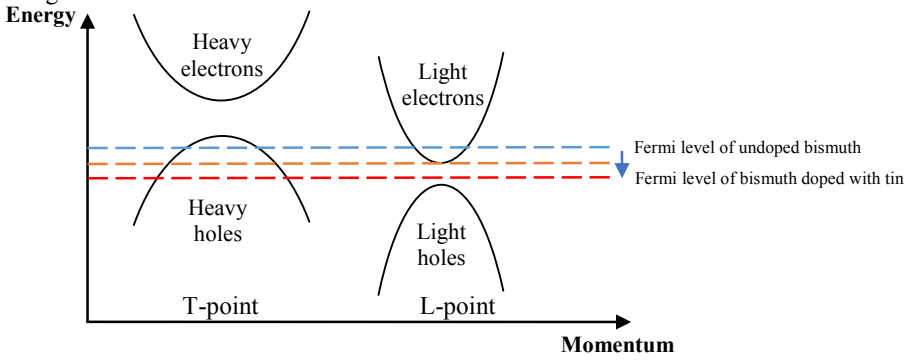


Fig. 7. Simplified band structure of bismuth-tin alloys.

Actually, in the studied temperature range there are three types of charge carriers in bismuth: L-band electrons, T-band heavy holes and L-band light holes [13]. In bismuth doped with tin the Fermi level is being shifted down what leads to fast rising both of L- and T-holes concentrations. Then, we should consider bismuth-tin diluted alloy as material with three different types of charge carriers. Calculation of concentrations and mobilities is difficult because it requires at least 6 equations for measured experimental characteristics and additional knowledge about band structure (such as precise value of Fermi energy in doped bismuth, Fermi energy temperature dependence and some suggestions about non-parabolicity of bands edges).

## 4. Conclusions

The dependences of resistivity, magnetoresistance, Hall effect and thermoEMF in the 4 – 300 K temperature range and in magnetic fields up to 8 T were studied for the $Bi_{1-x}Sn_x$ ($0 \le x \le 0.006$) diluted alloys produced by the melt spinning method. The observed decrease of conductivity and magnetoresistance with doping is explained in terms of charge carriers scattering on tin atoms, whereas the shift of the Hall and Seebeck coefficients to the range of positive values is connected with enhanced contribution of holes in the charge transport.

## References

[1] Issi J-P (edited by Rowe DM). Thermoelectrics Handbook: Macro to Nano. Thermoelectric properties of the Group V Semimetals. Boca Raton: Taylor and Francis; 2006.

[2] Poudel B, Hao Qing, Ma1 Yi, Lan Yucheng, M Austin, Yu Bo, Yan Xiao, Wang Dezhi, Muto A, Vashaee D, Chen X, Liu J, Dresselhaus MS, Chen G, Ren Z. High-Thermoelectric Performance of Nanostructured Bismuth Antimony Telluride Bulk Alloys. Science. 2008; 320:634-638.

[3] Srinivasan R, Gothard N, Spowart J. Improvement in thermoelectric properties of an n-type bismuth telluride ($Bi_2Se_{0.3}Te_{2.7}$) due to texture development and grain refinement during hot deformation. Mater Lett. 2010; 64:1772–1775.

[4] Richoux V, Diliberto S, Boulanger C, Lecuire JM. Pulsed electrodeposition of bismuth telluride films: Influence of pulse parameters over nucleation and morphology. Electrochim Acta. 2007;52: 3053–60.

[5] Li S, Toprak MS, Soliman HMA, Zhou J, Muhammed M, Platzek Dieter, Muhammet ST, Ziolkowski P, Nuller E. Effects of Annealing and Doping on Nanostructured Bismuth Telluride Thick Films. Chem Mater 2006; 8:3627–33.

[6] Menke EJ, Brown MA, Li Q, Hemminger JC, Penner RM. Bismuth telluride ($Bi_2Te_3$) nanowires: Synthesis by cyclic electrodeposition/stripping, thinning by electrooxidation, and electrical power generation. Langmuir 2006; 22:10564–74.

[7] Borca-Tasciuc D-A, Chen G, Prieto A, Martín-González MS, Stacy A, Sands T, Ryan MA, Fleurial JP. Thermal properties of electrodeposited bismuth telluride nanowires embedded in amorphous alumina. Appl Phys Lett Vol. 85, No. 24, pp. 6001–6003.

[8] Boettinger WJ, Perepezko JH, Liebermann HH. Rapidly solidified alloys: processes, structures, properties, applications. New York: Marcel Dekker Inc.; 1993.

[9] Shepelevich VG, Grechannikov EE. Connection between structure and physical pproperties of Bi-Sb alloys. Mozyr: MSPU; 2007.

[10] Oelsen W, Golucke KF. Thermodynamic Analysis, XI. Calorimetry and Thermodynamics of Bismuth-Tin Alloys. Arch Eisenhuttenw.1958;29:689-698.

[11] K Seeger. Semiconductor Physics: An Introduction. 6th ed. Berlin: Springer; 1997.

[12] Nakamura D, Murata M, Yamamoto H, Hasegawa Y, Komine T. Thermoelectric properties for single crystal bismuth nanowires using a mean free path limitation model. J Appl Phys 2011;110:053702.

[13] Towle L C, Cybriwsky A, Stajdohar R E. Light Holes in Bismuth-Tin Alloys. J Appl Phys 1966;38;668-672.